

Phase dependence of third-order harmonic generation in gases induced by two-color laser field

Congsen Meng (孟从森)^{1,†}, Pan Song (宋盼)^{1,†}, Zhihui Lyu (吕治辉)^{1*}, Xiaowei Wang (王小伟)¹, Dongwen Zhang (张栋文)¹, Zengxiu Zhao (赵增秀)¹, and Jianmin Yuan (袁建民)^{1,2}

¹Department of Physics, National University of Defense Technology, Changsha 410073, China

²Department of Physics, Graduate School of China Academy of Engineering Physics, Beijing 100193, China

*Corresponding author: lvzhihui@nudt.edu.cn

Received December 2, 2022 | Accepted February 8, 2023 | Posted Online May 6, 2023

We experimentally demonstrate third-harmonic generation (THG) in gases ionized by a femtosecond laser pulse superimposed on its second-harmonic (SH). The mechanism of THG has been investigated, and it demonstrates that a third-order nonlinear process dominates at low pump intensity. Asymmetric third-harmonic (TH) spectra are observed at different time delays in two color fields, which are attributed to the process of the four-wave mixing (FWM) of the broad spectrum of pump pulses. A joint measurement on the terahertz (THz) and the TH is performed. It reveals that the optimized phase for the THG jumps from 0 to 0.5π as the pump intensity increases, which is different from the THz being a constant, and indicates that the THG arises from the nonlinearity of the third-order bound electrons to the tunnel-ionization current.

Keywords: third-harmonic generation; THz.

DOI: [10.3788/COL202321.050201](https://doi.org/10.3788/COL202321.050201)

1. Introduction

The laser-gas nonlinear interaction induced by two-color femtosecond pulses has received considerable attention both experimentally and theoretically^[1-5]. The phase difference between two-color laser fields allows for effective access to coherently control the electronic wavepacket dynamics in atoms and molecules and leads to a wealth of phase-dependent quantum interference effects^[6,7]. Currently, two-color laser mixing in gas or solid has also been widely used to achieve high-intensity light sources, such as terahertz (THz) emission and high-harmonic generation (HHG). Up to now, the mechanism of THz emission is still under debate. Initially, THz generation was interpreted as a four-wave mixing process^[8], in which the third-order nonlinearity of a gas medium was verified to be too small to explain the measured terahertz field strength. Then, a non-perturbative plasma current model was proposed by Kim *et al.*^[9], where THz emission originates from a directional electron current produced by photoionization in a temporally asymmetric laser field arising from two-color laser pulses. For the mechanism of the HHG, it is widely accepted as being attributed to electron rescattering, which can be qualitatively understood by the well-known three-step model^[10]. Additionally, for HHG, it is of fundamental interest to investigate the generation of the low-order harmonics, in particular third-harmonic generation (THG) in two-color laser fields. From the single-atom perspective, THG is considered as nonlinear parametric conversion, mainly by a direct

THG channel, $3\omega = \omega + \omega + \omega$, and a four-wave mixing (FWM) channel, $3\omega = 2\omega + 2\omega - \omega$, in which the optimal phase delay [corresponding to a maximal third-harmonic (TH) yield] should be zero because its nonlinear coefficients are always considered to be real without resonance^[11]. To pursue high conversion efficacy of the THG, the strong pump laser is normally focused to ensure strong ionization of the gas medium, in which THG yield is considered to be dominated by the nonperturbative nonlinear response of free electrons, i. e., the tunnel ionization current^[12]. Experimental and theoretical studies have both demonstrated that the THG yield of a one-color laser field in air is determined by various characteristics, including laser intensity, pulse duration, focusing conditions, air pressure, etc^[13,14]. The underlying mechanism for an intense laser pulse propagating over long distances in optical media is the dynamic interplay between the Kerr self-focusing due to the nonlinear refractive index and the defocusing due to a low-density electron plasma^[15-18]. Compared to the case of the one-color laser field, the two-color laser field with phase delay becomes more complicated by the accurate determination of the relative phase delay. Recently, the dependence of the THG mechanism on the pump intensity has been theoretically investigated by a numerical simulation based on the time-dependent unidirectional pulse propagation equation^[19]. However, to the best of our knowledge, there is an overall lack of experimental investigation regarding the optimized phase delay of the THG

in gases induced by a two-color field at various pump laser intensities.

In this Letter, we report an experimental investigation on THG in the gases induced by two-color laser field. First, THGs via the direct channel and the FWM channel have been investigated, respectively. Then, employing a relative phase monitor, the variations of optimized phases for THz and TH generation have been obtained at different pump intensities based on the synchronous measurements of THz and THG.

2. Experimental Setup

The optical source is a 1 kHz commercial Ti:sapphire femtosecond amplification system that can deliver 25 fs pulses with the energy of 1.6 mJ. As sketched in Fig. 1, the fundamental pulse passes through a beta barium borate (BBO) crystal to generate a few tens of milliwatts of second-harmonic (SH). A two-color Mach-Zehnder (MZ) interferometer is utilized to accurately control the relative phase between the two pulses with a pair of fused-silica wedges in the path of the fundamental beam. In both paths, broadband half-wave plates are used to tune the pulse intensities with a broadband polarizer placed after the interferometer. The spatially and temporally overlapped two-color pulses are focused into a vacuum chamber to generate the THz and the TH emissions by using an off-axis parabolic mirror with the focal length of 200 mm. The THz is separated from the laser beams with a pierced off-axis parabolic mirror and then focused on a deuterated triglycine sulphate (DTGS) detector. The TH is filtered out with a reflecting UV filter and detected with a UV photodiode. In the residual pump path, a collinear interferometer is used to monitor the variation of the relative phase, in which another beta BBO crystal is utilized to achieve the interference between the newly frequency-doubled and the primary SH fields. The alpha BBO crystal is used to compensate the phase lag between the fundamental and SH pulses, and the orthogonally-polarized SH pulses are projected to a specific angle through a polarizer to achieve a distinct interference^[20,21].

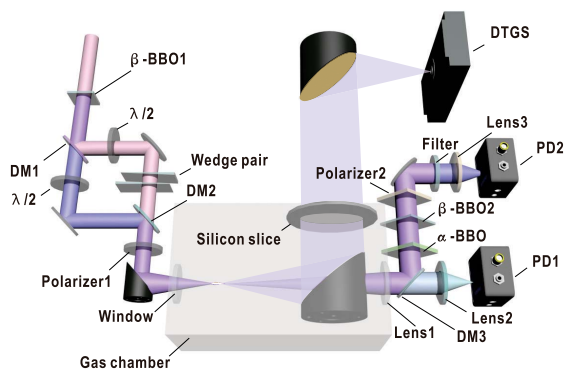


Fig. 1. Experimental setup for the synchronous measurements of the THz and TH emission. DM, dichroic mirror; PD, photodiode detector.

3. Results and Discussions

First, we carry out the experiments to study the THG from the direct and the FWM channel, respectively. To investigate the direct THG channel alone, the BBO crystal is removed in the experiment. Pump energy thresholds are presented for the three types of gases, as shown in Fig. 2(a). According to the previous studies, the phases of the TH generated before and after the focus cannot match well for the existence of the Gouy phase shift. The efficiency of the TH generation remains very low until the focusing condition has been alerted by self-focusing or gas ionization^[14], which is consistent with the observation that the threshold increases with the ionization probability ($\text{Ar} > \text{N}_2 > \text{He}$). Below the thresholds, no TH emissions can be detected with the photodiode sensitivity. The inset in Fig. 2(a) shows the TH yield as a function of the gas pressure at a fundamental pulse energy of 400 μJ . At low pressures, the square root of the TH intensity is linear as related to the gas pressure, and the TH yield can be considered as a coherent synthesis of the atom or molecule emissions. The critical pressure of Ar and N_2 corresponds to the occurrence of the intensity clamping, which is determined by the dynamic equilibrium between Kerr self-focusing and plasma-induced defocusing effects^[22,23].

To study the FWM channel, we measure the pump energy dependence of the TH generation as varying the time delay of the two-color pulses in argon at a pressure of 1000 mbar, where the full-width at half-maximum (FWHM) process dominates. Note that the distinct interference fringes are clearly observed, as shown in Fig. 2(b). The TH yield can be considered as a joint contribution of the direct channel, the FWM channel, and their interference, even though the fundamental pulse energy is quite lower than the threshold shown in Fig. 2(a). The contribution of the direct channel to the TH yield can be obtained at the time delay of the complete separation of the two-color laser field, and the interference can be eliminated by averaging the TH

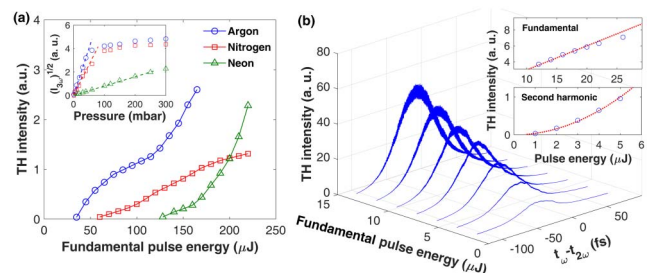


Fig. 2. (a) Measured TH intensity versus the fundamental pulse energy at a pressure of 1000 mbar in argon, nitrogen, and neon. According to the measured beam waist radius, the pulse energy of 100 μJ corresponds to the peak intensity of about $5 \times 10^{13} \text{ W/cm}^2$. The insert shows the square root of the TH intensity versus the gas pressure at a fundamental pulse energy of 400 μJ in argon, nitrogen, and neon. (b) TH intensity as a function of the pulse time delay and fundamental pulse energy at an SH pulse energy of 1 μJ . The insert shows the TH intensity versus the fundamental pulse energy at an SH pulse energy of 1 μJ and the SH pulse energy at a fundamental pulse energy of 1 μJ , respectively.

intensity over the interference cycle. Here, we assume that the full overlap of the two-color pulses gives the maximal TH yield and removes the influence of the direct channel by eliminating the period modulation mathematically. At low pump intensities, the relations between the TH yield and pump intensities shown in the insert of Fig. 2(b) agree well with the prediction of the FWM theory. As the fundamental beam intensity increases up to the threshold of the direct channel, a small deviation can be observed. It should be noted that, unlike the direct channel, the fundamental beam intensity shows no threshold for the THG via the FWM.

Next, employing a relative phase monitor, we carry out the experiment of synchronous measurements for the THz and the TH generation, since both the THz and the TH generation processes are intrinsically involved and highly phase sensitive. To suppress the influence of the macroscopic effects, a low pressure of 10 mbar and weak pump intensities of 100 μJ for the fundamental pulse and 5 μJ for the SH pulse are set. Figure 3(a) shows the THz and the TH intensities as adjusting the pump delay. The obtained curve envelopes for the THz and the TH present a similar pattern, and the Fourier analysis of the TH curve, shown in Fig. 3(b), indicates a period modulation of 0.67 fs, as well as that of THz emission, which is consistent with the previous experiment^[8,11]. Figure 3(c) shows the normalization modulation at three different time delays: -50 fs, 0 fs, and 50 fs, and curves are obtained by normalizing the intensity and fitted by sinusoidal functions. When two pump pulses are fully overlapped, as shown in the middle panel of Fig. 3(c), the THz modulation lags 0.2π behind the TH modulation, which reveals that the optimized relative phase for the THz and the TH is about 0.8π and zero, respectively. Actually, it is challenging to accurately determinate the absolute relative phase zero experimentally. Therefore, it is worthwhile investigating the intensity modulation versus the relative phase delay when two pulses are partially overlapped, as shown in the top and bottom panels of Fig. 3(c). With different time delays, the phase lag between the

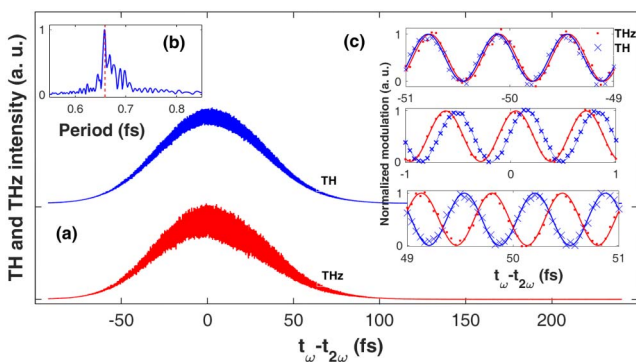


Fig. 3. Synchronous measurements for the THz and the THG. (a) The measured THz and TH intensities as functions of the time delay between the fundamental and the second harmonic pulses. (b) The Fourier analysis of the TH curve in (a). (c) The comparison of the phase-dependent intensity modulation between the THz and the TH at three different time delays: -50 fs, 0 fs, and 50 fs.

THz and the TH varies, and it reveals that the generation mechanisms of the two emissions can be distinct. For the low-intensity pulses, the TH and the THz are mainly attributed to the nonlinear response of the bound electrons and the free electrons, respectively^[9,24]. To further study the mechanism of the TH, the TH spectra at different pump delays are shown in Fig. 4 by replacing the UV photodiode with a spectrometer. Figure 4(b) shows that the two pulses are in perfect temporal overlap, the intensities of the different frequency components of the TH vary synchronously with the relative phase, and the spectrum presents a single-peak structure. Figures 4(a) and 4(c) show that the two pulses delay at -40 fs and 40 fs, respectively. An apparent asynchronous modulation and double-peak spectra can be observed, which is introduced by the chirped TH emission via the FWM channel. According to the FWM theory, the TH emission can be expressed as (fundamental harmonic, SH, and TH are denoted by ω_1 , ω_2 , and ω_3 , respectively)

$$E_{\omega_3} \propto \int d\omega_2 \int d\omega_2' \int \eta^{(3)} E_{\omega_2} E_{\omega_2'} E_{\omega_1} e^{i(\varphi_2 + \varphi_2' - \varphi_1)} d\omega_1, \quad (1)$$

where E and φ represent the electric-field vector and phase, respectively, and $\eta^{(3)}$ is the third-order susceptibility. For a specific frequency component, ω_3 of the TH emission, is satisfied with $\omega_3 = \omega_2 + \omega_2' - \omega_1$, where ω_2' is another frequency component of the SH. Supposing the phase of the SH is invariable, the frequency components of the fundamental pulse would vary in the phase following $\delta\varphi = (\omega_2 - \omega_1)\omega_1$ as the pump delay changes. The femtosecond pulse has a broad spectrum. Thus, in the case of a complete overlap, the additional relative phase would be zero. While in the case of an incomplete overlap, the different frequency components vary asynchronously, and the relative phase variation would increase with the departure of the pulse overlap, which leads to a chirped TH emission.

Finally, in order to study the dependence of the THz mechanism on the pump intensity, the optimized THz and TH yield

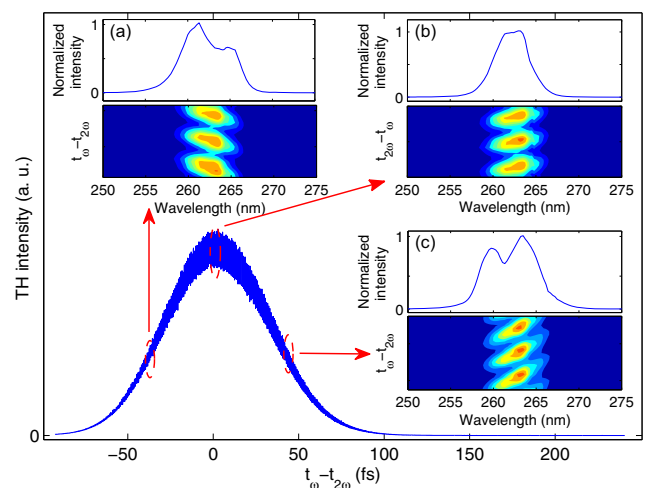


Fig. 4. TH spectra obtained at three different time delays: (a) -40 fs, (b) 0 fs, and (c) 40 fs.

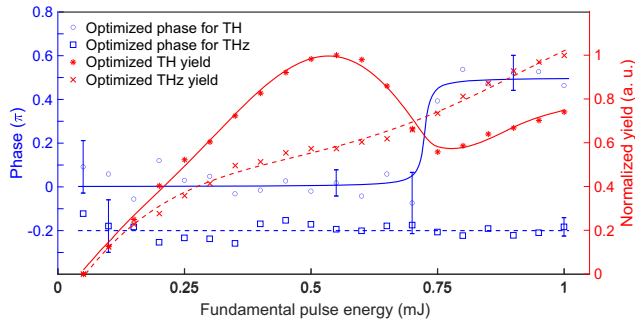


Fig. 5. The blue curves show the optimized phase for the TH (circles) and the THz [squares] (left axis), and the red curves show the optimized TH (asterisks) and the THz [crosses] yield (right axis).

and the optimized phase for the THz and the TH generation versus the fundamental pulse intensity are presented. The SH pulse energy of 50 μJ and gas pressure of 1 mbar are set to ensure the response of the DTGS detector and suppress the influence of macroscopic effects, respectively. The red curves in Fig. 5 show that the THz yield increases with the fundamental pulse energy while the TH yield increases to a maximum, decreases with a further increase of the fundamental energy, and then increases again at a pump energy of around 0.75 mJ. As discussed in the theoretical study of the TH mechanism^[14], in the intensity regime below the ionization threshold, the nonlinear response of the bound electrons dominates the THG process, and the third-order nonlinearity, $\eta^{(3)}$, increases with the pump intensity in the intensity regime of the tunneling ionization. On one hand, the effective third-order susceptibility decreases if a neutral gas is ionized. On the other hand, the density of the free electrons rises nearly stepwise at every half-cycle of the laser field, and the acceleration of the laser-induced photocurrent gives birth to the TH, i.e., the nonlinear response of the free electrons dominates the THG process^[25,26]. This argument is verified by investigating the optimized phase for the THz and the TH, as shown in the blue curves in Fig. 5. Here, the optimized phases are extracted as the pump delay approaches a perfect overlap, and the optimized phase for the TH generation at low pump intensities is supposed to be zero. It can be seen that the optimized phase for the THz generation is almost independent of the pump intensity and remains at about -0.2π (equivalent to 0.8π) within the experimental accuracy. However, the optimized phase for the TH generation, remains at zero at low pump intensities, where the FWM process dominates. As the pump intensity increases to be around 0.75 mJ, which almost coincides with the turning point of the TH yield, the optimized phase sharply rises up to 0.5π , and the THG is dominated by the tunnel ionization current.

4. Conclusion

In summary, we experimentally studied the mechanism of the THG as changing the fundamental laser intensity with a

two-color laser field. In the low-intensity regime, it is found that the THG originates from a third-order nonlinear process, that is, direct and FWM channels, which has been experimentally demonstrated, respectively, and the interference of these two channels has been verified. With a relative phase monitor, a joint measurement of the THz and the TH emissions was carried out precisely by varying the phase delay in attosecond precision. If the two pump pulses are incompletely overlapped, then the TH spectrum exhibits an asymmetric pattern arising from the FWM process with a broad spectrum of pump pulses. Furthermore, the dependence of the optimized THG yield and the optimized phase of the fundamental intensity is experimentally investigated, as well as that of the THz. As the pump intensity increases, the THG arises from the nonlinearity of the third-order bound electrons to the tunnel-ionization current, which is consistent with the theory and experiments^[27-29]. Our research provides further understanding of the mechanism of THG in gases and facilitates generating an efficient TH source for applications.

Acknowledgement

This work was supported by the National Key Research and Development Program of China (No. 2019YFA0307704), the National Natural Science Foundation of China (Nos. 11974425 and 11974426), and the National Safety Academic Fund (No. U1830206).

[†]These authors contributed equally to this work.

References

1. D. G. Arbó, C. Lemell, S. Nagele, N. Camus, L. Fechner, A. Krupp, T. Pfeifer, S. D. López, R. Moshhammer, and J. Burgdörfer, "Ionization of argon by two-color laser pulses with coherent phase control," *Phys. Rev. A* **92**, 023402 (2015).
2. H. Du and N. Yang, "Effect of gas species on THz generation from two-color lasers," *Chin. Opt. Lett.* **11**, 063202 (2013).
3. Z. Zhou, D. Zhang, Z. Zhao, and J. Yuan, "Terahertz emission of atoms driven by ultrashort laser pulses," *Phys. Rev. A* **79**, 063413 (2009).
4. Y. Jia, L. Guo, S. Hu, X. Jia, D. Fan, R. Lu, S. Han, and J. Chen, "Time-energy analysis of the photoionization process in a double-XUV pulse combined with a few-cycle IR field," *Chin. Opt. Lett.* **19**, 123201 (2021).
5. W. Yang, Y. Lin, X. Chen, Y. Xu, H. Zhang, M. Ciappina, and X. Song, "Wave mixing and high-harmonic generation enhancement by a two-color field driven dielectric metasurface [Invited]," *Chin. Opt. Lett.* **19**, 123202 (2021).
6. C. A. Mancuso, K. M. Dorney, D. D. Hickstein, J. L. Chaloupka, J. L. Ellis, F. J. Dollar, R. Knutt, P. Grychtol, D. Zusin, C. Gentry, M. Gopalakrishnan, and M. M. Murnane, "Controlling nonsequential double ionization in two-color circularly polarized femtosecond laser fields," *Phys. Rev. Lett.* **117**, 133201 (2016).
7. S. Heck, M. Han, D. Jelovina, J.-B. Ji, C. Perry, X. Gong, R. Lucchese, K. Ueda, and H. J. Wörner, "Two-center interference in the photoionization delays of Kr_2 ," *Phys. Rev. Lett.* **129**, 133002 (2022).
8. X. Xie, J. Dai, and X.-C. Zhang, "Coherent control of THz wave generation in ambient air," *Phys. Rev. Lett.* **96**, 075005 (2006).
9. K. Y. Kim, A. J. Taylor, J. M. Glowina, and G. Rodriguez, "Coherent control of terahertz supercontinuum generation in ultrafast laser-gas interactions," *Nat. Photonics* **2**, 605 (2008).

10. P. B. Corkum, "Plasma perspective on strong field multiphoton ionization," *Phys. Rev. Lett.* **71**, 1994 (1993).
11. H. Xu, W. Chu, Y. Liu, W. Liu, H. Xiong, Y. Fu, J. Yao, B. Zeng, J. Ni, S. L. Chin, Y. Cheng, and Z. Xu, "Third-harmonic generation in relative-phase-controlled two-color laser field," *Appl. Phys. B* **104**, 909 (2011).
12. R. A. Ganeev, M. Suzuki, M. Baba, H. Kuroda, and I. A. Kulagin, "Third-harmonic generation in air by use of femtosecond radiation in tight-focusing conditions," *Appl. Opt.* **45**, 748 (2006).
13. C.-J. Zhu, Y.-D. Qin, H. Yang, S.-F. Wang, and Q.-H. Gong, "Third-order harmonic generation in atmospheric air with focused intense femtosecond laser pulses," *Chin. Phys. Lett.* **18**, 57 (2001).
14. F. Théberge, N. Aközbek, W. Liu, J.-F. Gravel, and S. L. Chin, "Third harmonic beam profile generated in atmospheric air using femtosecond laser pulses," *Opt. Commun.* **245**, 399 (2005).
15. S. Backus, J. Peatross, Z. Zeek, A. Rundquist, G. Taft, M. M. Murnane, and H. C. Kapteyn, "16-fs, 1- μ J ultraviolet pulses generated by third-harmonic conversion in air," *Opt. Lett.* **21**, 665 (1996).
16. Y. Tamaki, K. Midorikawa, and M. Obara, "Phase-matched third-harmonic generation by nonlinear phase shift in a hollow fiber," *Appl. Phys. B* **67**, 59 (1998).
17. N. Aközbek, A. Iwasaki, A. Becker, M. Scalora, S. L. Chin, and C. M. Bowden, "Third-harmonic generation and self-channeling in air using high-power femtosecond laser pulses," *Phys. Rev. Lett.* **89**, 143901 (2002).
18. H. Yang, J. Zhang, J. Zhang, L. Z. Zhao, Y. J. Li, H. Teng, Y. T. Li, Z. H. Wang, Z. L. Chen, Z. Y. Wei, J. X. Ma, W. Yu, and Z. M. Sheng, "Third-order harmonic generation by self-guided femtosecond pulses in air," *Phys. Rev. E* **67**, 015401(R) (2003).
19. U. Sapaev, A. Husakou, and J. Herrmann, "Combined action of the bound-electron nonlinearity and the tunnel-ionization current in low-order harmonic generation in noble gases," *Opt. Express* **21**, 25582 (2013).
20. A. N. Chudinov, Y. E. Kapitzky, A. A. Shulginov, and B. Y. Zel'dovich, "Interferometric phase measurements of average field cube $E_{\omega}^2 E_{2\omega}^2$," *Opt. Quantum. Electron.* **23**, 1055 (1991).
21. J. Dai, N. Karpowicz, and X.-C. Zhang, "Coherent polarization control of terahertz waves generated from two-color laser-induced gas plasma," *Phys. Rev. Lett.* **103**, 023001 (2009).
22. J. Bernhardt, W. Liu, S. L. Chin, and R. Sauerbrey, "Pressure independence of intensity clamping during filamentation: theory and experiment," *Appl. Phys. B* **91**, 45 (2008).
23. Y.-Y. Tu, C. Meng, X. Sun, H.-Z. Wu, P. Song, C.-S. Meng, X.-W. Wang, Z.-Y. Zhou, Z.-H. Lyu, D.-W. Zhang, Z. X. Zhao, and J.-M. Yuan, "Enhancement of terahertz radiation from a filament by using circularly polarized two-color laser fields," *J. Opt. Soc. Am. B* **39**, A83 (2022).
24. V. A. Andreeva, O. G. Kosareva, N. A. Panov, D. E. Shipilo, P. M. Solyankin, M. N. Esaulkov, P. Martínez, A. P. Shkurinov, V. A. Makarov, L. Bergé, and S. L. Chin, "Ultrabroad terahertz spectrum generation from an air-based filament plasma," *Phys. Rev. Lett.* **116**, 063902 (2016).
25. D. Jang, R. M. Schwartz, D. Woodbury, J. Griff-McMahon, A. H. Younis, H. M. Milchberg, and K.-Y. Kim, "Efficient terahertz and Brunel harmonic generation from air plasma via mid-infrared coherent control," *Optica* **6**, 1338 (2019).
26. K. Zhang, Y. Zhang, X. Wang, T.-M. Yan, and Y. H. Jiang, "Continuum electron giving birth to terahertz emission," *Photon. Res.* **8**, 760 (2020).
27. K.-Y. Kim, "Generation of coherent terahertz radiation in ultrafast laser-gas interactions," *Phys. Plasmas* **16**, 056706 (2009).
28. T. He, Y. Zhang, J. J. Zhao, X. Wang, Z. Shen, Z. Jin, T.-M. Yan, and Y. Jiang, "Third-order harmonic generation in a bi-chromatic elliptical laser field," *Opt. Express* **29**, 21936 (2021).
29. K. Zhang, Y. Zhang, X. Wang, Z. Shen, T.-M. Yan, and Y. H. Jiang, "Experimental evidence for terahertz emission of continuum electrons in the dual-color laser field," *Opt. Lett.* **45**, 1838 (2020).